COMPUTER METHODS IN MATERIALS SCIENCE

2020, vol. 20, no. 4, 157–164
https://doi.org/10.7494/cmms.2020.4.0737

The influence of coolant velocity on the local heat transfer coefficient during steel quenching

Artur Szajding[1]*, Andrzej Gołdasz[2], Tadeusz Telejko[1]

[1] AGH University of Science and Technology, Faculty of Metals Engineering and Industrial Computer Science, Department of Heat Engineering and Environment Protection, al. Mickiewicza 30, 30-059 Krakow, Poland.
[2] AGH University of Science and Technology, Faculty of Energy and Fuels, Department of Thermal and Fluid Flow Machines, al. Mickiewicza 30, 30-059 Krakow, Poland.

Abstract

The results of the calculations of the local heat transfer coefficient HTC and a heat flux HF on the face of a cylindrical sample made of 1.0503 steel are presented. The sample was cooled from a temperature of approx. 930°C in a mineral oil having a temperature equal to 50°C. The experiments were performed for three speeds of the oil stream (0.2 m/s, 0.4 m/s and 0.6 m/s). The oil stream was directed perpendicularly to the cooled surface. The temperature of each sample was measured with 4 thermocouples and recorded with a frequency of 10 Hz. The maximum values of HTC always occurred in the axis of the sample and were in the range of 8000 to 10,000 W/(m^2 ·K). The results are presented in the form of useful graphs showing the dependence of HTC and HF on the surface temperature for various velocities of cooling oil. The calculations were made with self-developed software using the inverse solution of the boundary heat conduction problem.

Keywords: inverse method, heat transfer coefficient, boundary condition, quenching

1. Introduction

Heat treatment of metal alloys is a widely used process aimed at obtaining appropriate mechanical properties by the material by controlled shaping of their metallographic structure. In addition, it must be ensured that strains and residual stresses are kept at minimum values.

One of the most popular ways of heat treatment is quenching, which consists of heating steel to a high temperature, sometimes exceeding 1000°C, and then cooling it in a controlled manner. In order to achieve the required cooling rates, it is often necessary to use a liquid as the cooling medium. The phenomena of heat transfer between the liquid and the cooled surface are very complex and, in most cases, are related to the phase change of the coolant. In addition, the extremely difficult operating conditions associated with metal processing technologies impose a number of specific requirements on the fluids used. For this reason, water and its solutions as well as mineral oils are commonly used. The classic method of cooling with liquid is a process in which the material is immersed in a large tank with a cooling liquid. In this case, the movement of the liquid in the tank is an effect of free convection forces. Sometimes, in order to intensify the heat transfer, the liquid is mechanically stirred. In the heat treatment of geometrically small elements, special immersion methods are also used, in which a stream of cooling liquid directly hits the cooled surface, causing augmentation of heat transfer, the degree of which depends, among others, on the velocity of the liquid flow.

* Corresponding author: artur.szajding@agh.edu.pl
ORCID ID's: 0000-0001-5559-0771 (A. Szajding), 0000-0002-0746-1112 (A. Gołdasz), 0000-0002-0382-4051 (T. Telejko)

In the available literature, there are many studies on heat transfer during immersion cooling of steel. Sugiantoa et al. (2009) conducted research using cylindrical steel samples. The sensors for temperature measurement were placed at some points of the volume selected in such a way as to be representative of the zones formed on the sample surface, in which a homogeneous value of the heat transfer coefficient was assumed. The experiments were performed during cooling in stationary oil and cooling with oil stirring at the speed of 0.3 m/s and 0.7 m/s.

The study of heat transfer during cooling cylindrical sample made of austenitic steel heated to the initial 850°C was presented by Taraba et al. (2012). After equalization of the temperature in the entire volume, the sample was placed in a tank with Isorapid 277HM oil and cooled in an oil propelled by a stirrer. The two-dimensional axial-symmetric heat conduction in the sample was considered.

Research on steel ring immersion cooling was performed by Sahai and Aceves (2001). The ring was cooled in stationary and moving oil. The movement of oil in a vertical direction was induced by a stream generator. On the surface of the ring, arbitrarily defined zones were distinguished in which the boundary conditions were calculated separately.

The two-dimensional inverse problem of heat transfer at the side surface of a sample during immersion cooling has been investigated by Kim and Oh (2001). A cylinder-shaped sample, made of S45C steel (AISI-SAE type 1045), was heated in the furnace to approx. 500°C for the time necessary to equalize the temperature inside it. Then it was placed in a cooling medium, which was air flowing in a sheath at a known speed of 3.9 m/s or in a water tank in such a way that the axis of the sample was perpendicular to the direction of fluid flow. The air movement was forced by the fan, and the water movement – by natural convection and the boiling process. The aim was to determine the two-dimensional distribution of the heat transfer coefficient on the surface taking into account its change around the circumference of the cylinder.

Hernández-Morales et al. (2011) performed studies of heat transfer during cooling steel cylindrical samples in moving water. The samples were heated in a furnace to a temperature of over 900°C, placed in a vertical tube made of plexiglass, and immersed in a stream of flowing water. The movement of water was forced by a pump, and its flow was measured with a rotameter. On the basis of temperature measurements at individual points, the boundary conditions on the surface were determined using the inverse solution of the one-dimensional axisymmetric heat conduction problem.

The problems of heat transfer during immersion cooling are also the subject of extensive research in relation to non-iron alloys. The heat transfer during immersion cooling with the use of the inverse solution of the one-dimensional boundary problem was studied by Buczek (2004) and Buczek and Telejko (2004). For the tests, they used the cylindrical sensor made of bronze (60% Cu, 40% Zn). The sensor was heated to 500°C, 550°C, and 600°C and cooled in water having temperature equal to 20°C, 50°C, 80°C and 99.5°C (boiling temperature).

In another publication, the same authors (Buczek & Telejko, 2013) presented studies of immersion cooling of samples made of INCONEL 600 alloy taking into account the movement of the coolant near the hot surface. Two types of mineral oils and a polymer coolant were investigated. The probe was heated to 850°C in a resistance furnace. After equalizing the temperature profile inside the sample, it was immediately immersed in the movable or stagnant coolant having various but steady in time, temperatures.

Trujillo and Wallis (1989) performed heat transfer studies during cooling of a disk-shaped sample made of INCONEL 718 alloy. The disk was heated in a furnace to an initial temperature of approximately 1180°C, and then placed horizontally in an oil tank. From the solution of the inverse problem, changes in the heat flux density in time in separate zones of the upper and lower surfaces and on the side surface were determined.

Examples of research for alloys of other metals, e.g. aluminium, are the works (Cui et al., 2019) and (Kopun et al., 2014).

The above-mentioned studies consider selected parameters of the heat transfer processes that affect the intensity of cooling, including the flow rate of the cooling medium and its temperature. Most of them take into account only the average value of the heat transfer coefficient, and only some of them also take into account the heat transfer on the cooled surface in local terms. This means that it is required to divide the sample geometry into zones in which heat fluxes or heat transfer coefficients were averaged. The mathematical model adopted in this study allows for the determination of the local value of the heat transfer coefficient depending on the geometric coordinates without the need to initially divide the cooled surface into predetermined sub-areas.

2. Problem formulation

In order to solve the equation of heat conduction, the correct definitions of the initial and boundary conditions are required. The biggest research problem arises in the determination of the local heat transfer coefficient on the cooled surface.

In this study, the identification of the boundary conditions on the surface of the heated charge is based on the solution of the inverse heat conduction problem (IHCP).

The heat conduction model was based on the solution of the heat conduction equation in cylindrical coordinates (Cengel, 2011) with the use of the finite element method (FEM):

$$\lambda\left[\frac{\partial^2 T}{\partial r^2}+\frac{1}{r}\frac{\partial T}{\partial r}+\frac{\partial^2 T}{\partial z^2}\right]=\rho c\frac{\partial T}{\partial \tau} \quad (1)$$

where: T – temperature; τ – time; λ – thermal conductivity; c – heat capacity; ρ – density; r, z – cylindrical coordinates.

The variable temperature field on the cooled surface of the material $T(r, z, \tau)$ obtained as a result of solving equation (1) should meet the boundary conditions. They are written in the form of Fourier's law:

$$\dot{q}(r,\tau)=h(r,\tau)\cdot(T_s-T_p) \quad (2)$$

where: $\dot{q}$ – heat flux density; $h(r,\tau)$ – heat transfer coefficient; T_s – surface temperature; T_p – ambient temperature [K].

The two-dimensional axisymmetric heat conduction is assumed, where the heat transfer with the coolant occurs only on one of the cylinder's front surfaces. The heat losses through the remaining external surfaces (the side surface and the second front surface) were calculated, taking into account the convective and radiation heat exchange in the gap between the surfaces of the sample closed within the shield and the inner surface of the shield:

$$h_{gap}=\frac{\sigma(T_s^2+T_w^2)(T_s+T_w)}{\frac{1}{\varepsilon_s}+\frac{A_s}{A_w}\left(\frac{1}{\varepsilon_w}-1\right)}+\frac{\lambda_{gap}}{\delta} \quad (3)$$

where: h_{gap} – heat transfer coefficient in the gap, σ – Stefan–Boltzmann constant; T_s, T_w – temperature of the side/bottom (uncooled) surface of the sample and casing surface, respectively; ε_s, ε_w – sample and casing surface emissivity, respectively; A_s, A_w – sample and casing surface area, respectively; λ_{gap} – thermal conductivity of the gap; δ – gap thickness.

The inverse solution assumes a general form of an approximating function of the HTC distribution on the cooled surface *versus* time τ, and the specific parameters of this function are determined minimizing the error norm, which is the sum of the squares of the differences between measured – $t_{ij}^{mea}(\tau)$ and calculated – $t_{ij}^{inv}(p_i,\tau)$ temperatures, respectively:

$$E(p_i)=\frac{1}{M\cdot MP}\sum_{i=1}^{M}\sum_{j=1}^{MP}\left(\frac{t_{ij}^{mea}-t_{ij}^{inv}}{t_{ij}^{mea}}\right)^2 \quad (4)$$

where: $E(p_i)$ – error norm; p_i – vector of unknown (searched) parameters used in the function, which defines HTC distribution along a sample radius; M – number of temperature sensors; MP – number of measurements.

The variable matrix method, which utilizes Broyden–Fletcher–Goldfarb–Shanno (BFGS) updating technique has been used to minimize the objective function (Fletcher, 1987).

It has been assumed that the HTC distribution at the cooled surface can be approximated as a function of sample radius by the third-degree polynomial.

A detailed description of the FEM model, the inverse model, and sensitivity tests are presented in the paper (Cebo-Rudnicka et al., 2016).

3. Methodology of experimental research

The measurements were performed on the test stand shown schematically in Figure 1. The heating furnace allows the samples to be heated up to approx. 1200°C. Heating can take place in an inert atmosphere or in the air. The oil velocity can vary from 0 m/s to 1 m/s, and the oil temperature can be set from 25°C to 100°C. The design of the test stand enables cooling with an oil stream directed perpendicularly or parallel to the cooled surface.

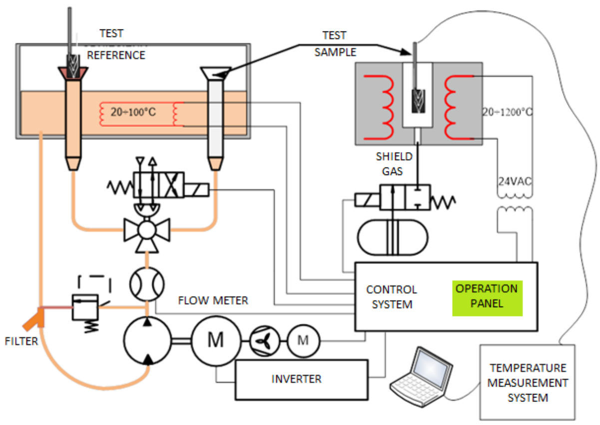

Fig. 1. Schematic drawing of the immersion cooling laboratory system

Experimental measurements were made for a cylindrical sample made of 1.0503 steel. A sample with a diameter and length of 20 mm was additionally placed in a cylindrical casing with a wall thickness of 0.5 mm in order to limit heat losses from surfaces, which were not cooled with oil. Figures 2 and 3 show a photograph of the sample and the arrangement of the thermocouples in the sample. In the space between the sample and the cylindrical sheath a ceramic fibre insulation material was placed. The temperature of the sample was measured with four K-type thermocouples with a sheath diameter of 1 mm. Three of them were located $L = 2$ mm below the cooled surface of the sample (in axis and at a radius of 5 mm and 8 mm). The fourth thermocouple was located in the axis of the sample at a distance of $L = 18$ mm from the cooled surface.

Fig. 2. The steel sample

a) b)

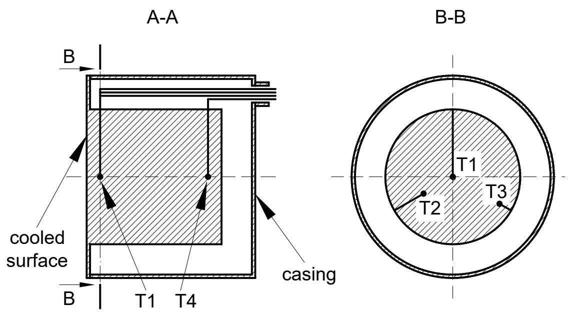

Fig. 3. Distribution of temperature measurement points in the sample: a) longitudinal section; b) cross-section

During the measurements, the sample was heated to a temperature of approx. 930°C, then placed in the holder located in the cooling chamber and cooled with oil at 50°C. Measurements were made for three oil speeds: 0.2 m/s, 0.4 m/s and 0.6 m/s. The oil stream was directed perpendicular to the plane of the cooled sample. The temperature was recorded with a data logger at a frequency of 10 Hz.

4. Results and discussion

Figure 4 shows an example of the temperature measurements for an oil velocity of 0.2 m/s, and Figure 5 shows a comparison of the temperature at point T_1 for oil velocities of 0.2 m/s, 0.4 m/s and 0.6 m/s. It was observed that the temperatures measured at the points T_2 ($r = 5$ mm) and T_3 ($r = 8$ mm) had a similar course. In the sample axis (point T_1, $r = 0$ mm) the measured temperatures are slightly higher, and at the point which is located much farther from the cooled surface T_4 ($r = 0$ mm, $L = 18$ mm), the recorded temperatures are naturally the highest. For the remaining oil cooling rates, the trend is the same.

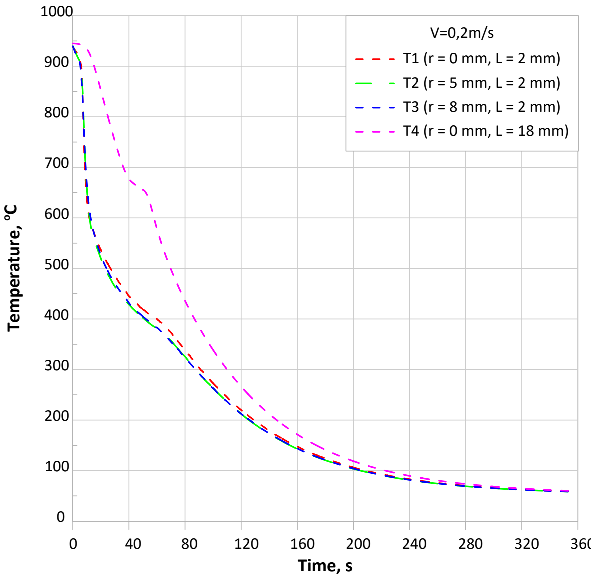

Fig. 4. Temperature at selected points for oil velocity $V = 0,2$ m/s

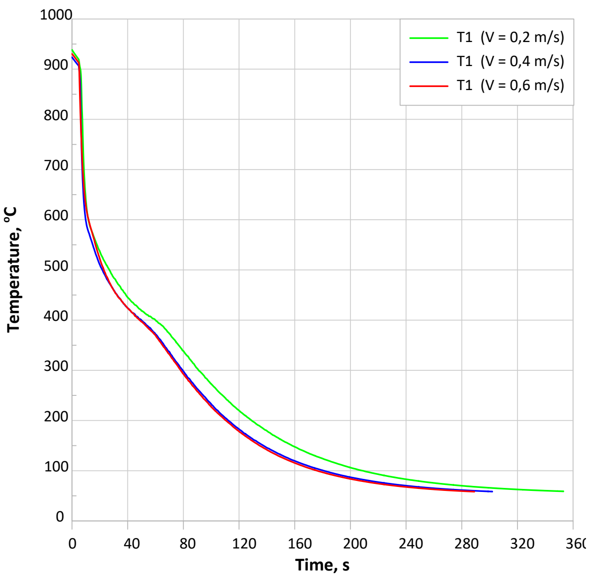

Fig. 5. Temperature measurements at point T_1 for various oil velocities

Figures 6 and 7 show exemplary experimentally measured temperatures and results of inverse calculations for an oil speed of 0.2 m/s. The coincidence at points T_1, T_2 and T_3 is very good. A greater discrepancy appears in the case of the temperature at point T_4, which lies far from the cooled surface. In this case, the greatest temperature difference is equal to 33.35 K after 49.4 s of cooling. Nevertheless, the average value of the temperature discrepancy for the entire measurements recorded by this sensor is 2.09 K only.

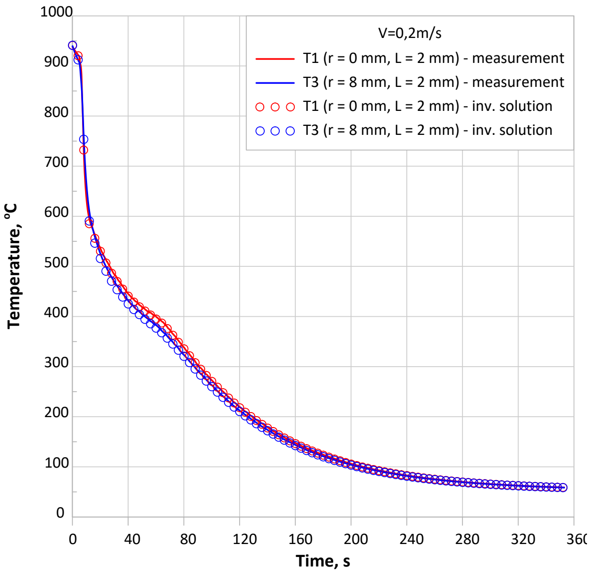

Fig. 6. Measured and numerically calculated temperature at points T_1 and T_3

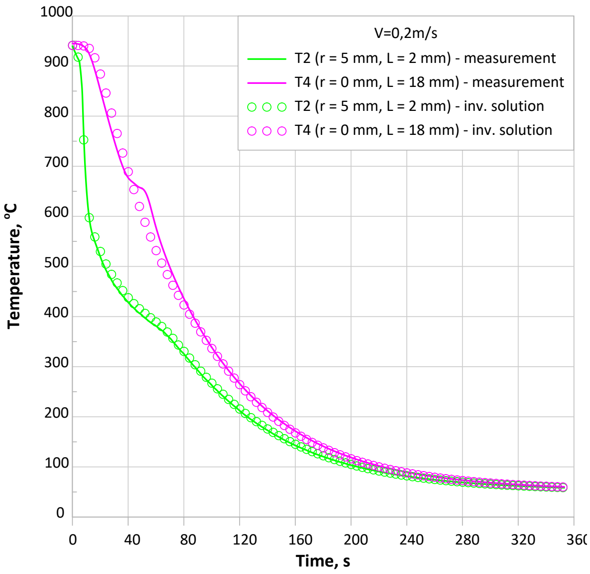

Fig. 7. Measured and numerically calculated temperature at points T_2 and T_4

Figures 8 and 9 show a comparison of the HTC on the cooled surface at $r = 0$ mm for various oil speeds as a function of time and surface temperature. Figure 8 has been truncated to 24 s due to the fact that the dynamic change of HTC occurs in a narrow time range between 4 s and 14 s. The entire course of HTC variation depending on the oil velocity is shown in Figure 10. It can be seen that with increasing oil velocity the maximum value of HTC also increases. For an oil velocity of 0.2 m/s, the maximum of HTC value was almost 8000 W/(m^2·K), for 0.4 m/s it was about 9300 W/(m^2·K), and for 0.6 m/s – about 10,000 W/(m^2·K), so subsequent increments of HTC$_{max}$ values are getting smaller. HTC maxima occur in the surface temperature range of 450÷550°C.

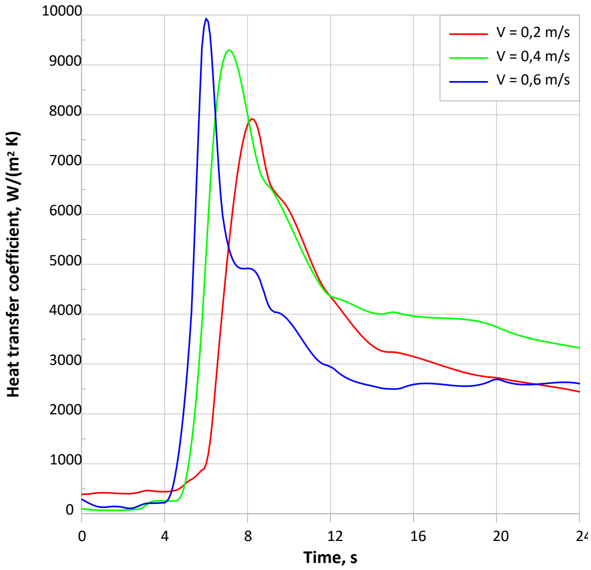

Fig. 8. HTC variations on the cooled surface at the sample axis ($r = 0$ mm) for various oil velocities up to 24 s from the start of cooling

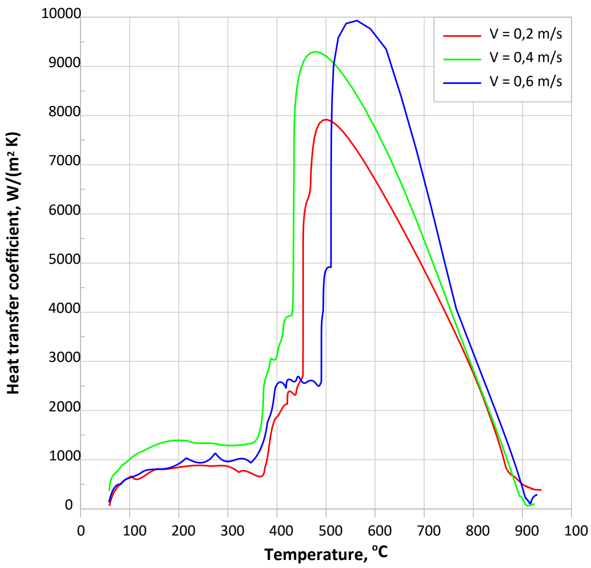

Fig. 9. Dependence of HTC on the surface temperature at the sample axis ($r = 0$ mm) for various oil velocities

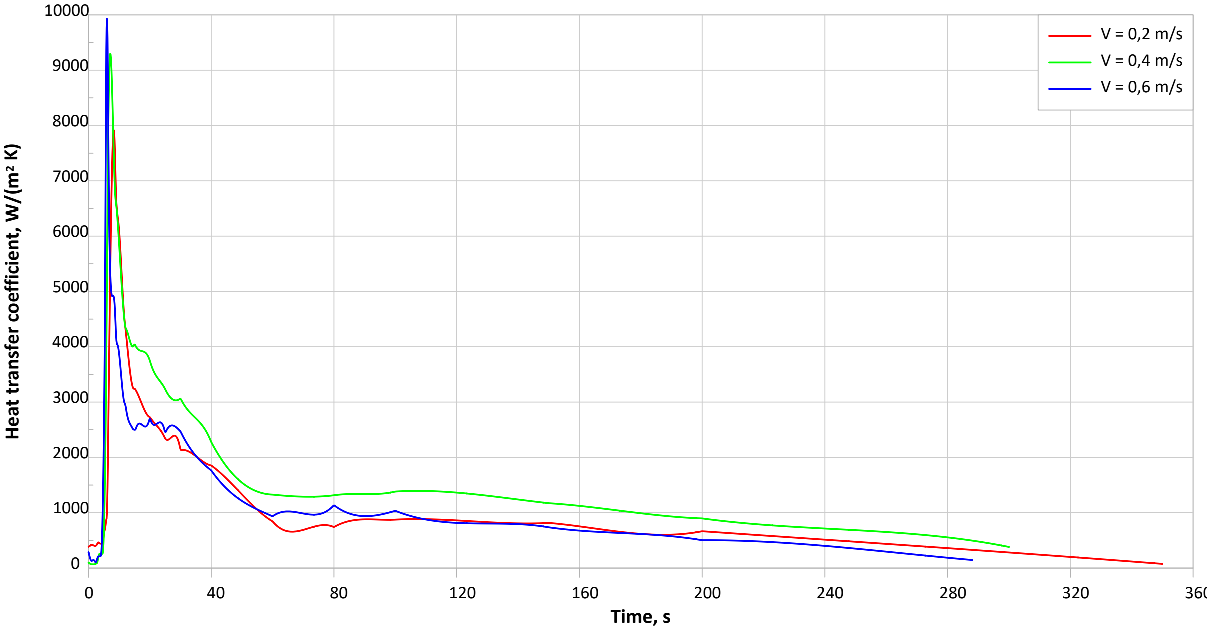

Fig. 10. HTC variations on the cooled surface at the sample axis ($r = 0$ mm) for various oil velocities

Figures 11 and 12 show the results of the HF calculations as a function of time on the cooled surface at the point $r = 0$ mm for various oil velocities. Figure 11 was also limited to 24 s, i.e. the period where dynamic changes in HF take place. As in the case of HTC, when the oil speed increases, the maximum value of the HF increases for the growing oil velocity and for 0.2 m/s, 0.4 m/s and 0.6 m/s is equal to about 3700 kW/m^2, 4300 kW/m^2 and 5300 kW/m^2, respectively. The occurrence of HF$_{max}$ is shifted towards higher temperatures in relation to HTC by approx. 100°C.

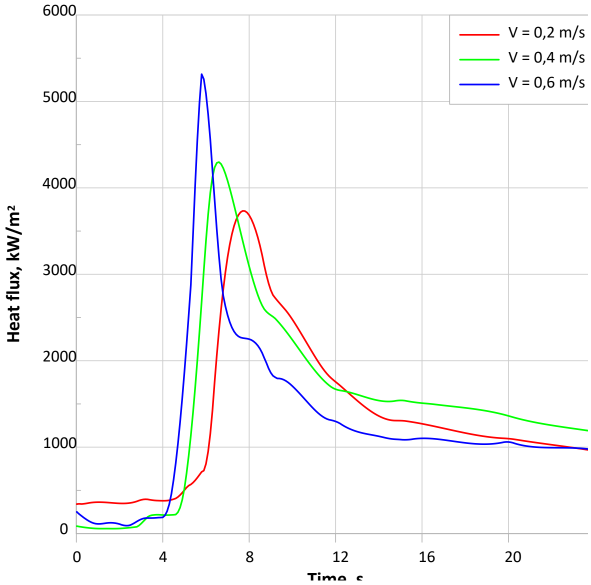

Fig. 11. HF variations on the cooled surface at the sample axis ($r = 0$ mm) for various oil velocities up to 24 s from the start of cooling

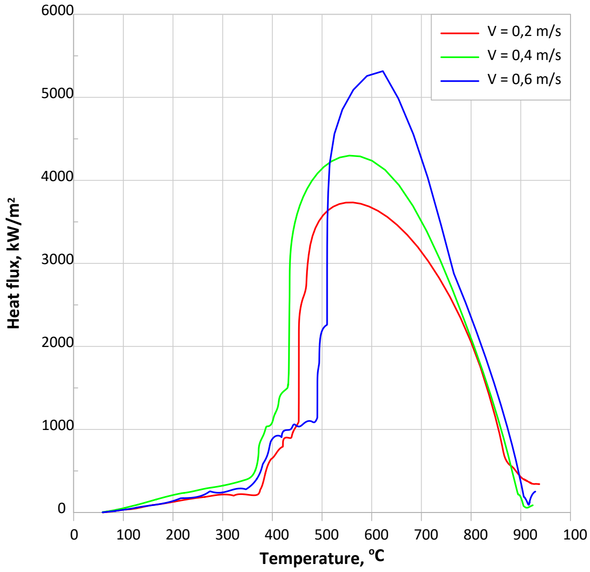

Fig. 12. Dependence of HF on the surface temperature at the sample axis ($r = 0$ mm) for various oil velocities

Figure 13 shows the HTC values at three points on the sample radius ($r = 0$, 5 and 8 mm) for an oil velocity of 0.2 m/s as a function of surface temperature. There are remarkable differences in the maximum values of HTC. The highest (almost 8000 W/(m$^2 \cdot$K)) occurs at the P_1 point lying in the centre of the cooled surface (in the sample axis). For the remaining points HTC$_{max}$ is equal to approx. 5500 W/(m$^2 \cdot$K) for $r = 5$ mm and approx. 3600 W/(m$^2 \cdot$K) for $r = 8$ mm. It is also clear that the occurrence of the HTC$_{max}$ moves towards the lower surface temperatures the closer to the axis of the sample.

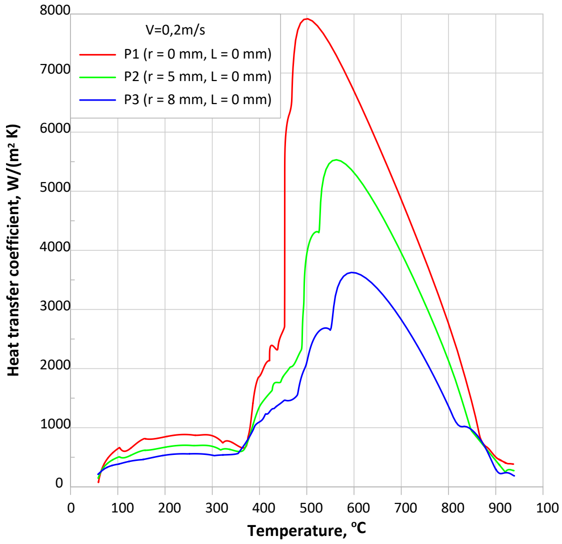

Fig. 13. Dependence of the heat transfer coefficient HTC on the temperature at selected points on the cooled surface for oil velocity 0.2 m/s

5. Summary

The tests and inverse calculations conducted allowed us to obtain local values of the heat transfer coefficient and the heat transfer flux on the cooled surface. The results of the tests and calculations lead to the following conclusions:

- The velocity growth of the cooling oil generates the increase of the local values, both HTC and HF. In the range of oil variability from 0.2 m/s to 0.6 m/s, the maximum local values of HTC occur in the temperature between 450°C and 550°C and fall within the range 8000÷10,000 W/(m^2·K). For the same oil velocities HF_{max} vary from approx. 3700 kW/m^2 to 5300 kW/m^2 and exist at the temperature of approx. 100°C higher. This may indicate the occurrence of the first boiling crisis at temperatures of 550°C÷620°C.
- The maximum values of the local HTC values were always found in the geometrical centre of the cooled surface for each test. For velocity of 0.2 m/s the HTC_{max} is almost 8000 W/(m^2·K) for r = 0 mm. The successive values decreased to about 5500 W/(m^2·K) for r = 5 mm and to about 3600 W/(m^2·K) for r = 8 mm. It was also found that the closer to the axis of the sample, the HTC_{max} moved towards the lower surface temperatures.

The results of numerical calculations were presented in the form of diagrams showing the dependence of the HTC and HF as a function of the surface temperature for various cooling oil velocities. The calculations were performed by the self-developed software that uses the inverse solution of the boundary heat conduction equation. The solution is characterized by a very good consistency between the calculated and the measured temperatures. A significant discrepancy appears only in the case of temperature at T_4 point, which lies a long distance from the cooled surface. In this case, the greatest temperature difference is 33.35 K occurring after 49.4 s of cooling time. Nevertheless, the mean value of the temperature error for all measurements at this point was 2.09 K.

Figures 4 and 7 clearly show a slowdown in temperature drop at T_4 point resulting from the thermal effects of phase transformation, which were not included in the mathematical model. These effects will be taken into account in further research. Experimental tests for other oil velocities and oil temperatures are also planned.

Acknowledgment

Work supported by statutory activities of the Faculty of Metals Engineering and Industrial Computer Science of AGH. Work no. 16.16.110.663.

References

Buczek, A. (2004). *Zastosowanie brzegowego zagadnienia odwrotnego do identyfikacji współczynnika przejmowania ciepła podczas chłodzenia.* Uczelniane Wydawnictwa Naukowo-Dydaktyczne AGH.

Buczek, A., & Telejko, T. (2004). Inverse Determination of Boundary Conditions During Boiling Water Heat Transfer in Quenching Operations. *Journal of Materials Processing Technology*, *155–156*, 1324–1329. https://doi.org/10.1016/j.jmatprotec.2004.04.192.

Buczek, A., & Telejko, T. (2013). Investigation of Heat Transfer Coefficient During Quenching in Various Cooling Agents. *International Journal of Heat and Fluid Flow*, *44*, 358–364. https://doi.org/10.1016/j.ijheatfluidflow.2013.07.004.

Cebo-Rudnicka, A., Malinowski, Z., & Buczek, A. (2016). The influence of selected parameters of spray cooling and thermal conductivity on heat transfer coefficient. *International Journal of Thermal Sciences*, 110, 52–64. https://doi.org/10.1016/j.ijthermalsci.2016.06.031.

Cengel, Y.A. (2011). *Heat Transfer. A Practical Approach*. McGraw Hill.

Cui, X., Wan, M., Ma, B., Wu, X., & Han, J. (2019). Quenching by immersion considering boiling heat transfer. *International Journal of Thermal Sciences*, *139*, 303–311. https://doi.org/10.1016/j.ijthermalsci.2019.01.039.

Fletcher, R. (1987). *Practical methods of optimization*. John Wiley & Sons.

Hernández-Morales, B., Vergara-Hernández, H.J., Solorio-Díaz, G., & Totten, G.E. (2011). Experimental and Computational Study of Heat Transfer During Quenching of Metallic Probes. In: A. Ahsan (ed.), *Evaporation, Condensation and Heat transfer* (pp. 49–72). InTech.

Kim, H.K., & Oh, S.I. (2001). Evaluation of Heat Transfer Coefficient During Heat Treatment by Inverse Analysis. *Journal of Materials Processing Technology*, *112*(2–3), 157–165. https://doi.org/10.1016/S0924-0136(00)00877-3.

Kopun, R., Škerget, L., Hriberšek, M., Zhang, D., Stauder, B., & Greif, D. (2014). Numerical simulation of immersion quenching process for cast aluminium part at different pool temperatures. *Applied Thermal Engineering*, *65*(1–2), 74–84. https://doi.org/10.1016/j.applthermaleng.2013.12.058.

Sahai, V., & Aceves, S.M. (2001). Determination of Heat Transfer During Gear Blank Quenching. *Heat Transfer Engineering*, *22*(4), 56–66. https://doi.org/10.1080/01457630118610.

Sugiantoa, A., Narazaki, M., Kogawara, M., & Shirayori, A. (2009). A comparative study on determination method of heat transfer coefficient using inverse heat transfer and iterative modification. *Journal of Materials Processing Technology*, *209*(10), 4627–4632. https://doi.org/10.1016/j.jmatprotec.2008.10.016.

Taraba, B., Duehring, S., Španielka, J., & Hajdu, Š. (2012) Effect of Agitation Work on Heat Transfer during Cooling in Oil ISORAPID 277HM. *Strojniški vestnik – Journal of Mechanical Engineering*, *58*(2), 102–106. https://doi.org/10.5545/sv-jme.2011.064.

Trujillo, D.M., & Wallis, R.A. (1989). Determination of heat transfer from components during quenching. *Industrial Heating*, *56*(7), 22–24.